Gold Bull (2012) 45:3–8
DOI 10.1007/s13404-012-0043-z

ORIGINAL PAPER

Tin-modified gold-based bulk metallic glasses

Shuo-Hong Wang · Tsung-Shune Chin

Published online: 16 February 2012

Abstract Tin was selected as a modifying element in low-gold-content (50 at.%) bulk metallic glasses (BMGs) aiming at developing alloys with cost-effective performance. New gold-based Au–Sn–Cu–Si alloys were fabricated by injection-casting into a copper mold. The as-cast BMG $Au_{50}Sn_6Cu_{26}Si_{18}$ with 18.6-karat gold and a diameter of 1 mm possessed a lower glass transition temperature (T_g) of 82°C (355 K), a lower liquid temperature of 330°C (603 K), and a super-cooled liquid region of 31°C. The viscosity range of this BMG $Au_{50}Sn_6Cu_{26}Si_{18}$ was from 10^8 to 10^9 Pa s measured at a low applied stress of 13 kPa. To compare the viscosity with different applied stresses, its viscosity clearly increased with applied stress below T_g but not so obvious above T_g. The low viscosity of this BMG $Au_{50}Sn_6Cu_{26}Si_{18}$ at around 102°C, which is very close to the boiling temperature of water (100°C), rendered easy thermal–mechanical deformation in a boiling water-bath by hand-pressing and tweezers-bending. Such a deformation capability in boiling water is beneficial to the further applications in various fields.

Keywords Gold-based alloys · Bulk metallic glasses · Glass transition temperature · Thermal mechanical analysis · Viscosity · Deformation capability

Electronic supplementary material The online version of this article (doi:10.1007/s13404-012-0043-z) contains supplementary material, which is available to authorized users.

S.-H. Wang · T.-S. Chin (✉)
Department of Materials Science and Engineering,
National Tsing Hua University,
No. 101, Section 2, Kuang-Fu Road,
Hsinchu 30013, Taiwan
e-mail: tschin@mx.nthu.edu.tw

T.-S. Chin
e-mail: tschin@fcu.edu.tw

T.-S. Chin
Center for Nanotechnology, Materials Science and Microsystems,
National Tsing Hua University,
No. 101, Sec-2, Kuang-Fu Road,
Hsinchu 30013, Taiwan

T.-S. Chin
Department of Materials Science and Engineering,
Feng Chia University,
No. 100, Wenhwa Road, Seatwen District,
Taichung 40724, Taiwan

Introduction

Pure gold is a precious metal and possesses the characteristics of luster, softness, malleability, and ductility. However, in its pure form, it is too soft to be used for monetary exchange and for producing jewelry materials. Thus, hardening of gold by alloying it with Cu, Ag, Ni, or other metals have been a common practice for a long time [1, 2]. Moreover, because of its superior thermal conductivity, excellent electrical conductivity, and high resistance to corrosion, gold has been widely applied in modern industries including IC electronics, aerospace, medicine, and dentistry [3]. Although pure gold and gold-based alloys with higher karats without toxic elements are useful and acceptable for the human body, the existence of grain boundaries in crystalline gold-based alloys is an ongoing concern with biomedical implants.

Metallic glass is amorphous in structure, containing no crystalline anisotropy, dislocation, grain boundary, or crystalline defects [4]. Bulk metallic glasses (BMGs) usually possess unique properties such as high strength and elasticity, increased hardness, good toughness, and excellent resistance to corrosion compared to their crystalline counterparts

[5, 6]. Since 1988, a large number of BMG systems have been developed notably those Mg- [7], La- [8], Zr- [9], Fe- [10], Pd- [11], Pt- [12], Ti- [13], Ni- [14], and Ca- [15] alloy systems. These BMGs exhibit large critical glass forming size and high thermal stability and hence reveal new possibilities for industrial applications.

In 1960, Klement et al. [5] synthesized the first amorphous alloy using the binary eutectic $Au_{82}Si_{18}$ composition, in thickness less than 50 μm. However, its poor glass-forming ability (GFA) has resulted in limited development over the past several decades. Schroers et al. exploited gold-based multi-component BMGs. These Au-based BMGs possessed a low glass transition temperature (T_g) of at most 128°C, good thermal stability at ambient temperature, and increased hardness, and they were easier to process. For Au–Ag–Pd–Cu–Si BMGs, the addition of Pd and Ag enhances GFA but they increase T_g [3]. On the other hand, Zhang et al. increased the gold content in Au–Ag–Cu–Si BMGs and resulted in a sharp decrease in T_g. The lowest reported T_g for an Au-based BMG is 66°C in the high-Au content composition $Au_{70}Cu_{5.5}Ag_{7.5}Si_{17}$ [16]. The above properties make Au-based BMGs useful for applications such as jewelry, micro-electromechanical systems (MEMS), electronics, nano-molding technologies [17, 18], and dentistry [19].

The purpose of this study is to explore new Au-based BMG composition with cost-effective performance. Composition design is to keep the gold content as low as possible, yet not less than 18 karats. We used tin as an inexpensive alloying element instead of palladium or silver. The performance of major concern is the thermal properties in particular the relationship between viscosity and deformation capability (processing characteristics) of such BMGs. More specifically, our ultimate goal is to develop a new Au-based BMG with low glass transition temperature which will facilitate processing capability to benefit further applications.

Experimental details

In this work, alloy ingots with nominal compositions $Au_{50}Sn_6Cu_{26}Si_{18}$, $Au_{50}Sn_6Cu_{24}Si_{20}$, and $Au_{50}Sn_9Cu_{23}Si_{18}$ were prepared by arc melting the mixtures of pure elements Au, Sn, Cu, and Si with purities of at least 99.9% under vacuum at 10^{-2} Torr. For homogeneity of the alloys, we melted the ingots six times for each composition. Bulk alloy rods with diameters of 1 mm were fabricated by conventional injection casting into a copper mold under an argon atmosphere. The structure of the as-cast rods was examined by X-ray diffractometry (XRD, Shimadzu XRD-6000) using Cu $K_{\alpha 1}$ radiation. The thermal properties were studied by a differential scanning calorimetry (DSC; PerkinElmer Diamond DSC) at a fixed heating rate of 20°C/min under flowing argon. To study the processing ability, we used a thermal mechanical analyzer (TMA; PerkinElmer Diamond TMA). The as-cast rods were cut into pieces, each with an aspect ratio of around 2 and polished at both ends. TMA measurements were performed with applied loads of 10 and 50 mN. We raised the temperature of the as-cast rods at a fixed heating rate of 10°C/min starting from room temperature to 200°C. The microstructure was observed on cross sections of the as-cast rods using a transmission electron microscope (TEM; JOEL 2010F) operating at an accelerating potential of 200 kV. Structural identification of the phases was carried out by conventional selected area electron diffraction (SAED).

Results and discussion

Figure 1 depicts the X-ray diffraction (XRD) patterns taken from the transverse cross sections of the as-cast 1-mm-diameter rods of $Au_{50}Sn_6Cu_{26}Si_{18}$, $Au_{50}Sn_6Cu_{24}Si_{20}$, and $Au_{50}Sn_9Cu_{23}Si_{18}$ alloys. The XRD results indicate that no obvious diffraction peaks could be identified for the $Au_{50}Sn_6Cu_{26}Si_{18}$ alloy, which shows a fully amorphous structure. The $Au_{50}Sn_6Cu_{26}Si_{18}$ BMG has a GFA capable of casting into amorphous rods of at least 1 mm in diameter and is the easiest to process of all our Au–Sn–Cu–Si quaternary alloys. The new Sn-added alloys show poor GFA when the Cu content decreased from 26 at.% (by being replaced by Si or Sn). This means that the increase in Si content is harmful to the formation of the quaternary Au–Sn–Cu–Si BMG. On the other hand, as Cu is partially substituted by Sn, the GFA also obviously decreases. We thus aimed to further investigate the BMG $Au_{50}Sn_6Cu_{26}Si_{18}$.

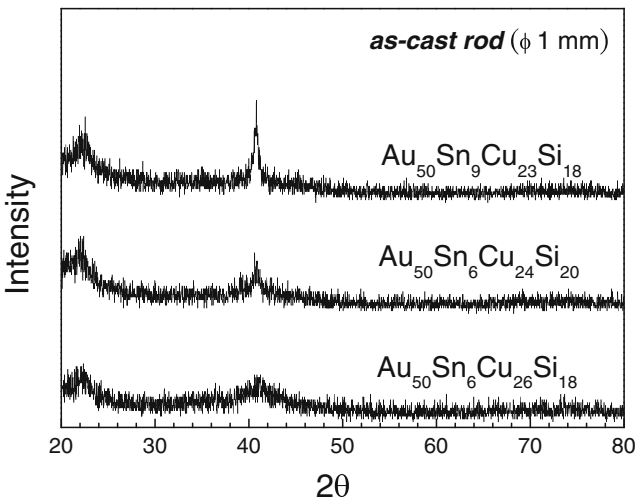

Fig. 1 X-ray diffraction patterns taken from cross sections of as-cast 1-mm diameter rods of $Au_{50}Sn_6Cu_{26}Si_{18}$, $Au_{50}Sn_6Cu_{24}Si_{20}$, and $Au_{50}Sn_9Cu_{23}Si_{18}$ alloys

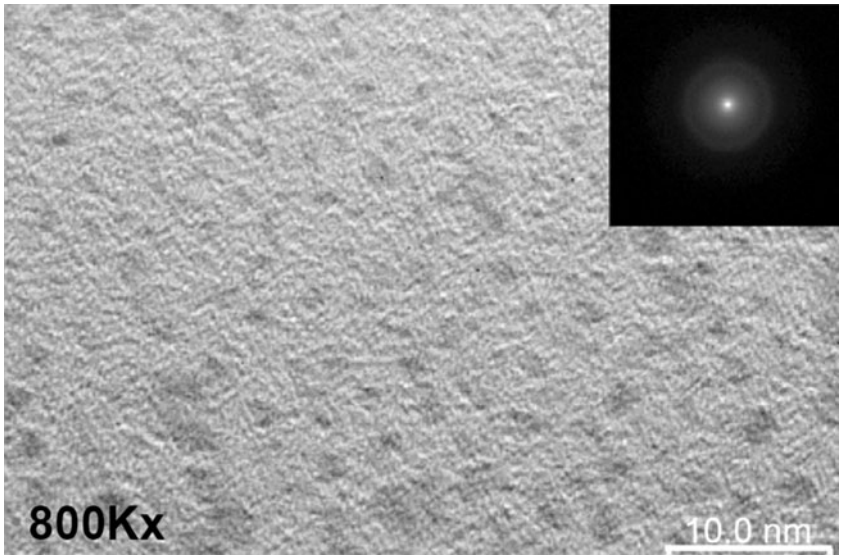

Fig. 2 Typical TEM image and selected area diffraction pattern (*SADP*) of specimen taken from as-cast 1-mm diameter rod of $Au_{50}Sn_6Cu_{26}Si_{18}$ alloy

The microstructure of the $Au_{50}Sn_6Cu_{26}Si_{18}$ as-cast BMG rod was studied by TEM (Fig. 2) together with a selected area diffraction pattern (SADP). The lack of diffraction spots or rings in the SADP indicates that the structure of the BMG $Au_{50}Sn_6Cu_{26}Si_{18}$ was amorphous even though there were slight contrasts in the matrix.

A typical DSC curve of the $Au_{50}Sn_6Cu_{26}Si_{18}$ as-cast BMG rod is shown in Fig. 3. The crystallization temperature T_x and T_g are 113°C and 82°C, respectively. The liquid temperature (T_l) of $Au_{50}Sn_6Cu_{26}Si_{18}$ BMG is 330°C. The calculated thermal criteria are the super-cooled liquid region (ΔT_x), 31 K; the reduced glass transition temperature (T_{rg}), 0.59; and the γ-factor 0.403. Although the ΔT_x of the $Au_{50}Sn_6Cu_{26}Si_{18}$ BMG was not as high as those reported in the literature [16], it was expected to be potential for easier processing below 100°C in hot water because of low T_g and moderate ΔT_x. Therefore, we carried out further study on its viscosity at elevated temperatures, as to be delineated later. Table 1 summarizes the thermal parameters of Au-based BMGs measured using the DSC. By comparing the results with those of other Au-based BMGs whose Au content 46–52 at.%, the T_g of our $Au_{50}Sn_6Cu_{26}Si_{18}$ BMG is obviously much lower than those of Au-based BMGs containing Pd and Ag. The ΔT_x (31°C) of $Au_{50}Sn_6Cu_{26}Si_{18}$ BMG is higher than that of BMG $Au_{46}Ag_5Cu_{29}Si_{20}$ (ΔT_x=25°C) but lower than that of Pd-containing BMG $Au_{49}Ag_{5.5}Pd_{2.3}Cu_{26.9}Si_{16.3}$ (ΔT_x=58°C). Among these Au-based BMGs, the most well known is the composition $Au_{49}Ag_{5.5}Pd_{2.3}Cu_{26.9}Si_{16.3}$. Despite its high T_g, this BMG has been widely used as the mold material in nano-imprint technology and in MEMS. Therefore, our BMG alloy, which has a lower T_g and does not contain Pd and Ag, is more cost-effective in similar applications.

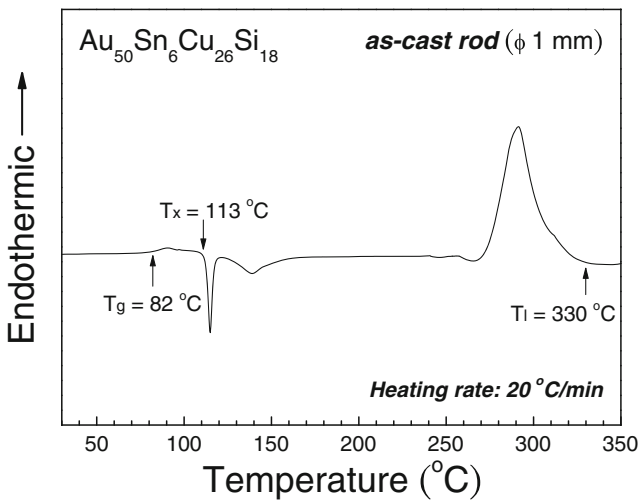

Fig. 3 Typical DSC curve of as-cast 1-mm diameter rod of $Au_{50}Sn_6Cu_{26}Si_{18}$ alloy

Thermal mechanical analysis (TMA) and differential TMA (DTMA) curves of the $Au_{50}Sn_6Cu_{26}Si_{18}$ as-cast BMG rod at an applied load of 50 mN are plotted in Fig. 4. The DTMA curve shows the differentiated results of displacement related to time. To exhibit the relationship between temperature and viscosity several parameters are defined. They are the onset temperature of viscous flow for the initial state (T_{onset}); the temperature corresponding to the lowest viscosity which is the viscosity of semi-steady state (T_{vs}); and the finishing temperature of viscous flow for the full crystallization state (T_{finish}). These are marked on the DTMA curve. From the DTMA curve, T_{onset}, T_{vs}, and T_{finish} are 84°C, 108°C, and 116°C, respectively. The values of T_{onset} and T_{finish} are very close to those of T_g (82°C) and T_x (113°C), respectively. TMA data and DSC data are almost the same for these two specific temperatures. The viscosity

Table 1 Thermal parameters of several Au-based BMGs found in the literature along with the values determined from this study [3]

Composition (at.%)	T_g (K)	T_x (K)	ΔT_x	T_l (K)	T_{rg}	γ	Ref.
$Au_{50}Sn_6Cu_{26}Si_{18}$	355	386	31	603	0.59	0.403	This study
$Au_{50}Cu_{33}Si_{17}$	383	405	22	679	0.56	0.381	[3]
$Au_{46}Ag_5Cu_{29}Si_{20}$	395	420	25	664	0.59	0.397	[3]
$Au_{52}Pd_{2.3}Cu_{29.2}Si_{16.5}$	393	427	34	651	0.6	0.409	[3]
$Au_{49}Ag_{5.5}Pd_{2.3}Cu_{26.9}Si_{16.3}$	401	459	58	644	0.62	0.439	[3]

of the $Au_{50}Sn_6Cu_{26}Si_{18}$ BMG can be evaluated according to the Stefan equation [20]:

$$\eta = \left(\frac{\sigma}{3\dot{\varepsilon}}\right)\left(1 + \frac{d_0^2}{8l_0^2(1+\varepsilon_n)^2}\right)^{-1}, \quad (1)$$

where σ is the stress (Pa), $\dot{\varepsilon}$ is the strain rate (s^{-1}), d_0 is the initial diameter of the specimen, l_0 is the initial length of the specimen, and ε_n the engineering strain (nominal strain). The stress is calculated by $\sigma = (F/A_0)(l/l_0)$, where F, A_0, and l are the applied loading force (mN), initial cross-sectional area of the specimen, and length after deformation, respectively. Calculated results are plotted in Fig. 5.

The curves in Fig. 5a and b show that the viscosity values of the $Au_{50}Sn_6Cu_{26}Si_{18}$ BMG are between 10^8 and 10^9 Pa s at an applied stress of 13 kPa, and 2×10^8 and 10^{10} Pa s at an applied stress of 65 kPa. The viscosity of the BMG $Au_{50}Sn_6Cu_{26}Si_{18}$ is in a range similar to that of the BMG $Au_{49}Ag_{5.5}Pd_{2.3}Cu_{26.9}Si_{16.3}$ (10^7–10^9 Pa s) obtained by Tang et al. [17]. However, the lower limit is relatively higher than those of BMGs $Mg_{65}Cu_{25}Gd_{10}$ and $Mg_{65}Cu_{25}Gd_{10}P_3$ (10^6–10^{10} Pa s) obtained by Chang et al. [20]. In addition, we observed that viscosity increases as increasing applied stress from 13 to 65 kPa. These tendencies are consistent with those reported by Chang et al. [21] for the BMG $Mg_{58}Cu_{31}Y_{11}$. In the literature, Tang et al. reported that the applied stress was in the range of 40–400 kPa or even higher for the BMG $Au_{49}Ag_{5.5}Pd_{2.3}Cu_{26.9}Si_{16.3}$ [17]. Hence, the applied flow stress of 13 kPa for the BMG $Au_{50}Sn_6Cu_{26}Si_{18}$ is relatively low [21, 22].

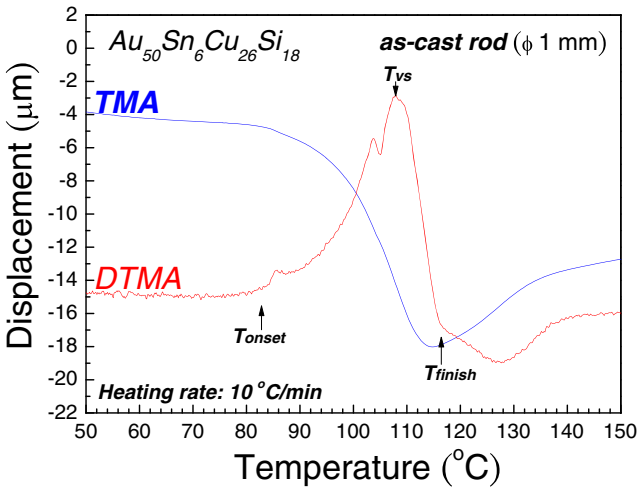

Fig. 4 TMA and DTMA curves of as-cast $Au_{50}Sn_6Cu_{26}Si_{18}$ BMG rod at the applied load of 50 mN

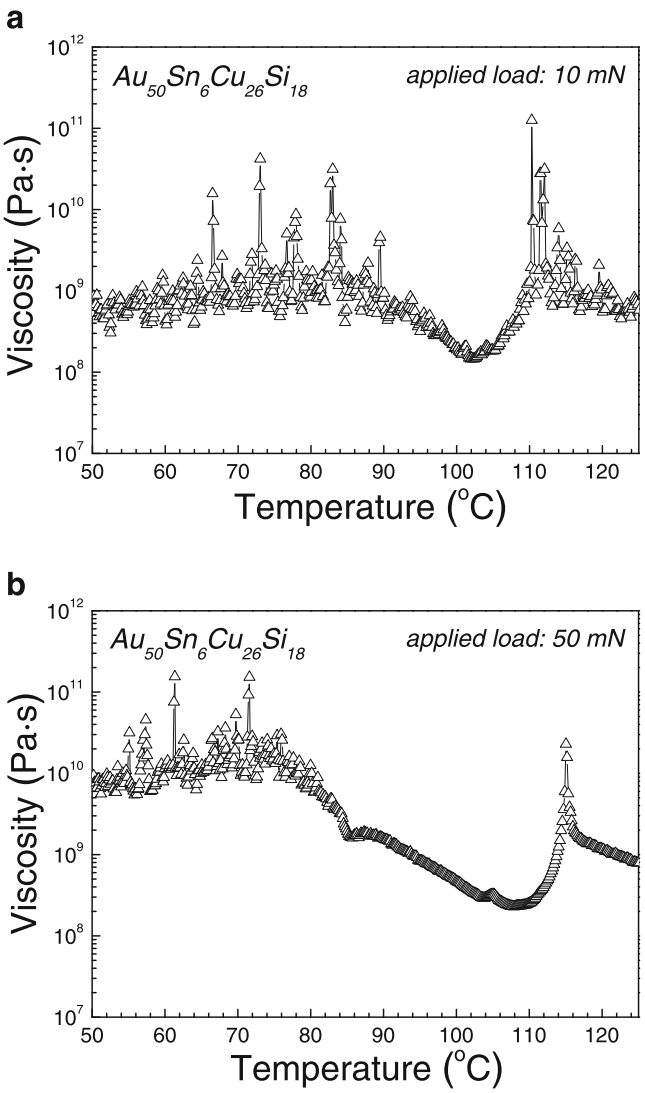

Fig. 5 Estimated viscosity of as-cast $Au_{50}Sn_6Cu_{26}Si_{18}$ BMG, measured under an applied load of **a** 10 mN (corresponding to 13 kPa) and **b** 50 mN (65 kPa)

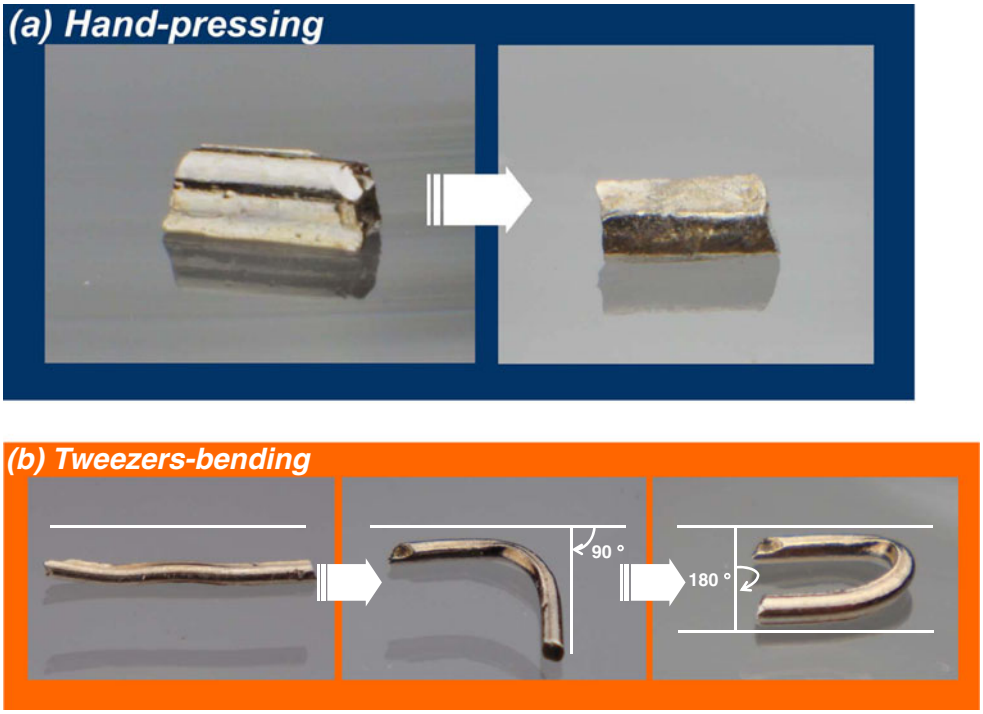

Fig. 6 Deformation capability of as-cast $Au_{50}Sn_6Cu_{26}Si_{18}$ BMG in the boiling water-bath by **a** hand-pressing and **b** tweezers-bending

In addition, the viscosity value is highly dependent on temperature. In fact, the much higher viscosity measured at 65 kPa is at a temperature much lower than 83°C, which is the TMA glass transition temperature. As the temperature becomes higher than 83°C, the viscosity soon declines to its minimum value. The viscosity decreases from 10^9 to 10^8 Pa s for both applied stresses of 13 and 65 kPa. Over this temperature range, the BMG $Au_{50}Sn_6Cu_{26}Si_{18}$ exhibits a typical viscosity of a Newtonian liquid. There exists a subtle difference in minimum viscosity values, 10^8 Pa s at 13 kPa and 2×10^8 Pa s at 65 kPa, and at different temperatures of the lowest viscosity (T_{vs}), 102°C at 13 kPa and 108°C at 65 kPa. This indicates that the applied stress does influence the measured viscosity to some extent. Above 113°C, the BMG no longer exhibits the viscosity that is characteristic of glassy materials, but instead shows the deformation characteristics of a rigid crystalline solid in responding to applied stress at elevated temperatures. These results indicate that the BMG $Au_{50}Sn_6Cu_{26}Si_{18}$ can have a viscous flow.

According to the result of viscosity, the proposed best temperature for thermal deformation is at 102°C, which is very close to the boiling temperature of water (100°C). Hence, we think it is possible to investigate the deformability of the as-cast $Au_{50}Sn_6Cu_{26}Si_{18}$ BMG, 1 mm in diameter, in boiling water-bath. Figure 6a and b exhibits the results of hand-pressed and tweezers-bent $Au_{50}Sn_6Cu_{26}Si_{18}$ BMG in boiling water-bath. It shows that rod-shaped $Au_{50}Sn_6Cu_{26}Si_{18}$ BMG can be pressed to be flattened, and can be bent to 90–180° repeatedly for several times without breaking or hardening. We did deformation out of the boiling water-bath and the BMG rod soon cracked. These are direct proofs that the BMG alloy deforms by a viscous flow mechanism in boiling water. Such a deformation capability in boiling water, which does not need a temperature controller to maintain isothermal condition, is very useful for application in various fields. These include but not limited to nano-imprint molds, dental prosthesis, jewelry, or MEMS devices.

Conclusions

In summary, we explored a cost-effective quaternary gold-based BMG $Au_{50}Sn_6Cu_{26}Si_{18}$ with a gold content of 18.6 karats in this research. This alloy retains a good GFA which renders possibility of inject-casting into BMG rod of at least 1 mm in diameter. This new Au-based BMG is characteristic of low glass transition (82°C), crystallization (113°C), and liquid (330°C) temperatures and a moderate super-cooled liquid region (ΔT_x, 31°C). Moreover, the $Au_{50}Sn_6Cu_{26}Si_{18}$ BMG exhibits a viscosity ranging from 10^8 to 10^9 Pa s measured under an applied stress as low as 13 kPa. The merit of its significant deformation capability at around 100°C (i.e., at the boiling temperature of water) renders easy and precise deformation without the use of a temperature controller. Based on these outstanding and cost-effective characteristics, the new BMG $Au_{50}Sn_6Cu_{26}Si_{18}$ will find extensive applications in molds for nano-imprinting, dental prosthesis, jewelry, and MEMS devices in the future.

Acknowledgment The authors are grateful to the National Science Council of the Republic of China for sponsoring this research under grant NSC 97-2221-E-035 -011-MY2.

References

1. Drummond IM (1987) The gold standard and international monetary system. Macmillan, New York
2. Vilar P, White J (1991) A history of gold and money. Verso, London
3. Schroers J, Lohwongwatana B, Johnson WL, Peker A (2005) Gold based bulk metallic glass. Appl Phys Lett 87:061912. doi:10.1063/1.2008374
4. Greer AL (1995) Metallic glasses. Science 267:1947–1953. doi:10.1126/science.267.5206.1947
5. Klement W, Willens RH, Duwez P (1960) Non-crystalline structure in solidified gold-silicon alloys. Nature 197:869–870. doi:10.1038/187869b0
6. Loffler JF (2003) Bulk metallic glasses. Intermetallics 11:529–540. doi:10.1016/S0966-9795(03)00046-3
7. Inoue A, Ohtera K, Kita K, Masumoto T (1988) New amorphous Mg–Ce–Ni alloys with high-strength and good ductility. Jpn J Appl Phys 27:2248–2251
8. Inoue A, Zhang T, Masumoto T (1989) Al–La–Ni amorphous-alloys with a wide supercooled liquid region. Mater Trans JIM 30:965–972
9. Inoue A, Zhang T, Masumoto T (1990) Zr–Al–Ni amorphous-alloys with high glass-transition temperature and significant supercooled liquid region. Mater Trans JIM 31:177–183
10. Lin CY, Tien HY, Chin TS (2005) Soft magnetic ternary iron–boron-based bulk metallic glasses. Appl Phys Lett 86:162501. doi:10.1063/1.1901808
11. Inoue A, Nishiyama N, Matsuda T (1996) Preparation of bulk glassy $Pd_{40}Ni_{10}Cu_{30}P_{20}$ alloy of 40 mm in diameter by water quenching. Mater Trans JIM 37:181–184
12. Schroers J, Johnson WL (2004) Highly processable bulk metallic glass-forming alloys in the Pt-Co-Ni-Cu-P system. Appl Phys Lett 84:3666–3668. doi:10.1063/1.1738945
13. Lin XH, Johnson WL (1995) Formation of Ti–Zr–Cu–Ni bulk metallic glasses. J Appl Phys 78:6514–6519. doi:10.1063/1.360537
14. Tien HY, Lin CY, Chin TS (2006) New ternary Ni-Ta-Sn bulk metallic glasses. Intermetallics 14:1075–1078. doi:10.1016/j.intermet.2006.01.042
15. Amiya K, Inoue A (2002) Formation, thermal stability and mechanical properties of Ca-based bulk glassy alloys. Mater Trans 43:81–84. doi:10.2320/matertrans.42.543
16. Zhang W, Guo H, Chen MW, Saotome Y, Qin CL, Inoue A (2009) New Au-based bulk glassy alloys with ultralow glass transition temperature. Scr Mater 61:744–747. doi:10.1016/j.scriptamat.2009.06.020
17. Tang TW, Chang YC, Huang JC, Gao Q, Jang JSC, Tsao CYA (2009) On thermomechanical properties of Au–Ag–Pd–Cu–Si bulk metallic glass. Mater Chem Phys 116:569–572. doi:10.1016/j.matchemphys.2009.04.032
18. Kumar G, Tang HX, Schroers J (2009) Nanomoulding with amorphous metals. Nature 457:868–872. doi:10.1038/nature07718
19. Lee SH, Lim IS, Cho MH, Pyo AR, Kwon YH, Seol HJ, Kim HI (2011) Age-hardening and overaging mechanisms related to the metastable phase formation by the decomposition of Ag and Cu in a dental Au–Ag–Cu–Pd–Zn alloy. Gold Bull 44:155–162. doi:10.1007/s13404-011-0021-x
20. Chang YC, Huang JC, Cheng YT, Lee CJ, Du XH, Nieh TG (2008) On the fragility and thermomechanical properties of Mg–Cu–Gd– (B) bulk metallic glasses. J Appl Phys 103:103521. doi:10.1063/1.2927459
21. Chang YC, Huang TH, Chen HM, Huang JC, Nieh TG, Lee CJ (2007) Viscous flow behavior and thermal properties of bulk amorphous $Mg_{58}Cu_{31}Y_{11}$ alloy. Intermetallics 15:1303–1308. doi:10.1016/j.intermet.2007.03.012
22. Jang JSC, Chang CF, Huang YC, Chiang WJ, Nieh TG, Liu CT (2009) Viscous flow and microforming of a Zr-base bulk metallic glass. Intermetallics 17:200–204. doi:10.1016/j.intermet.2008.07.019